Flow induces barrier and glycocalyx-related genes and negative surface charge in a lab-on-a-chip human blood-brain barrier model

Ana R Santa-Maria, Fruzsina R Walter, Ricardo Figueiredo, András Kincses, Judith Vigh, Marjolein Heymans, Maxime Culot, Peter Winter, Fabien Gosselet, András Dér, et al.

HAL Id: hal-03185580
https://univ-artois.hal.science/hal-03185580

Submitted on 18 Jul 2022

Flow induces blood-brain barrier and glycocalyx-related genes and negative surface charge in a lab-on-a-chip human culture model

Ana R. Santa-Maria[1,2,3], Fruzsina R. Walter[1,3], Ricardo Figueiredo[4,5], András Kincses[1,6], Judith Vigh[1,2], Marjolein Heymans[7], Maxime Culot[7], Peter Winter[4], Fabien Gosselet[7], András Dér[1], Maria A. Deli[1,*]

[1] Institute of Biophysics, Biological Research Centre, Temesvári krt. 62, H-6726, Szeged, Hungary

[2] Doctoral School of Biology, University of Szeged, Közép fasor 52, H-6726, Szeged, Hungary

[3] Department of Biotechnology, University of Szeged, Közép fasor 52., H-6726, Szeged, Hungary

[4] GenXPro GmbH, Altenhöferallee 3, D-60438, Frankfurt-Am-Main, Germany

[5] Johann Wolfgang Goethe University Frankfurt, Frankfurt-Am-Main, Germany

[6] Doctoral School of Multidisciplinary Medical Sciences, University of Szeged, Tisza Lajos körút 109., H-6725, Szeged, Hungary

[7] Univ. Artois, UR 2465, Laboratoire de la Barrière Hémato-Encéphalique (LBHE), F-62300 Lens, France

* Corresponding author:

Mária A. Deli,

Institute of Biophysics, Biological Research Centre, Temesvári krt 62, H-6726, Szeged, Hungary

Tel. +36-62-599602

e-mail: deli.maria@brc.hu

Running title: Flow induced changes in a human BBB model

Keywords: blood-brain barrier; gene sequencing; glycocalyx; lab-on-a-chip; surface charge

Abstract

Microfluidic lab-on-a-chip (LOC) devices allow the study of blood-brain barrier (BBB) properties in dynamic conditions. We studied a BBB model, consisting of human endothelial cells derived from hematopoietic stem cells in co-culture with brain pericytes, in an LOC device to study fluid flow in the regulation of endothelial, BBB and glycocalyx-related genes and surface charge. The highly negatively charged endothelial surface glycocalyx functions as mechano-sensor detecting shear forces generated by blood flow on the luminal side of brain endothelial cells and contributes to the physical barrier of the BBB. Despite the importance of glycocalyx in the regulation of BBB permeability in physiological conditions and in diseases, the underlying mechanisms remained unclear. The MACE-seq gene expression profiling analysis showed differentially expressed endothelial, BBB and glycocalyx core protein genes after fluid flow, as well as enriched pathways for the extracellular matrix molecules. We observed increased barrier properties, a higher intensity glycocalyx staining and a more negative surface charge of human brain-like endothelial cells (BLECs) in dynamic conditions. Our work is the first study to provide data on BBB properties and glycocalyx of BLECs in an LOC device under dynamic conditions and confirms the importance of fluid flow for BBB culture models.

Introduction

Due to the importance of the blood-brain barrier (BBB) in many systemic as well as central nervous system (CNS) diseases[1] improved *in vitro* models are crucial as research tools for the biomedical community. In the last decade, several *in vitro* BBB models have been developed using cell culture inserts representing static conditions and more complex lab-on-a-chip (LOC) devices.[2,3] Fluidic and microfluidic LOCs provide fluid flow and enable the study of BBB in a dynamic condition,[4,5] in contrast to static cell culture inserts.

The morphology of the BBB, the structure of brain endothelial cells (EC) connected by tight intercellular junctions (TJ) and that of surrounding pericytes, astroglia endfeet, perivascular microglia and neuronal processes are well described.[6] Recent advances in gene sequencing and single cell analysis led to better understanding of the molecular composition of cell populations of the brain including the cell types forming the BBB.[7,8] More complete lists of influx and efflux transporters, receptors and transport pathways are available for the different types of BBB cells which participate in providing nutrients for the CNS and also act as protection systems.[6,9] The BBB shields the CNS from toxins and pathogens but also participates in the pathomechanism of CNS injuries and neuroinflammation.[1,6]

In addition to physical defense mechanisms provided by TJs, and chemical protection by efflux pumps and BBB metabolic enzymes, the fourth major line of defense is the endothelial surface glycocalyx (ESG). Blood flow induces mechanical forces acting on the surface of ECs, which via mechanosensors, signaling pathways and gene expression, modulate endothelial morphology and function.[10,11] ESG is a sugar-protein matrix like layer covering the EC surface mainly composed of proteoglycans, glycoproteins, and glycosaminoglycans. Its unique location, composition and structure serves as a negatively charged physical barrier on the surface of ECs.[11] A recent *in vivo* study highlights the denser structure of glycocalyx of microvessel in the brain as compared to lung and heart, and associates it with brain EC protection as a defense component of the BBB.[12] Indeed, the surface charge of brain ECs is more negative than that of other vascular ECs, which was related to a higher level of negatively charged phosphatidylserine and phosphatidylinositol in their cell membrane,[13] in addition to the negative surface charge derived from the sulfate and sialic acid residues of the ESG.[10,14] The structural complexity and the negative surface charge of the ESG at the BBB not only provide an extra barrier on the EC, but also regulate the penetration of large molecules[15] and charged drugs or vectors to the CNS.[14,16] The protective role of ESG is well known

in the cardiovascular system, and damage of this surface layer was demonstrated in diseases and pathologies like atherosclerosis, ischemia and inflammation.[12,17] The characterization of ESG at the level of the BBB is incomplete and its importance is not fully understood.

Since LOCs provide more physiological conditions, in the present study we characterized a human BBB model composed of ECs derived from hematopoietic stem cells co-cultured with brain pericytes[18] in our microfluidic and microelectronic device.[5] Furthermore, our goal was to investigate the effect of fluid flow on gene expression of brain-like endothelial cells (BLECs) by in-depth massive analysis of cDNA ends sequencing (MACE-seq) with a focus on general endothelial, BBB-related and ESG-related genes. To confirm the results endothelial morphology, immunostaining of selected BBB proteins, lectin and immunostaining of ESG and surface charge measurements by laser Doppler velocimetry were performed. Our present work, together with our previous study revealing the importance of brain EC surface charge in the permeability of charged molecules,[16] draws the attention to ESG as a flow-regulated essential part of BBB models.

Material and Methods

Materials

All materials used in the study were purchased from Sigma-Aldrich, Hungary Ltd. (a subsidiary of Merck, Germany), unless otherwise indicated.

Cell culture

The *in vitro* BBB model, consisting of human endothelial cells (hEC) in co-culture with bovine brain pericytes, was described by Cecchelli *et al.* in 2014.[18] The isolation of stem cells required the collection of human umbilical cord blood, which was approved by the Hospital ethical committee (Béthune Maternity Hospital, Béthune, France). Informed consent was obtained from the infants' parents. The protocol was approved by the French Ministry of Higher Education and Research (CODECOH Number DC2011-1321). The study was conducted according to World Medical Association Declaration of Helsinki. The hECs were derived from CD^{34+} cord blood hematopoietic stem cells by a differentiation period of 15-20 days using $VEGF_{165}$.[18] After differentiation hECs were seeded in 0.2% gelatin coated culture dishes and kept in endothelial cell culture medium (ECM, Sciencell, USA) supplemented with 5 % fetal bovine serum (FBS), 1 % endothelial cell growth supplement (ECGS, Sciencell), and gentamycin (50 µg/ml). After

4

reaching confluency, hECs were gently trypsinized and 80×10^3 cells seeded into the polyester membrane of the lab-on-a-chip (LOC) device (Figure 1(b)), coated with Matrigel (BD Biosciences, USA). The LOC was built as described in our previous publication,[5] a brief protocol is provided in the Supplementary Methods. Bovine brain pericytes (PC) were cultured in 0.2% gelatin coated dishes in Dulbecco's modified Eagle's medium (DMEM, Life Technologies, Thermo Fisher Scientific, USA) supplemented with 20% FBS, 1% Glutamax (Life Technologies) and gentamicin (50 µg/ml). When cultures reached confluency, PCs were trypsinized and 25×10^3 cells were added to the bottom compartment of the LOC device coated with 0.2% gelatin (Figure 1(b)). During co-culture both compartments received endothelial medium. The LOC device with the cells was kept at 37°C in a humified atmosphere and 5% CO_2. For more details, see Supplementary Methods.

Dynamic culture conditions in the LOC device

To determine the importance of fluid flow on BLECs, the co-culture of BLECs with PCs lasted for 6 days under static condition (supplementary Figure S1) then 24 hours under dynamic condition (Figure 1(c)), and compared with cells which were kept under static condition for 7 days (for details see Supplementary Methods). Cell growth was monitored by phase contrast microscopy (MotiCam 1080, MoticEurope, Barcelona, Spain), since the transparency of the gold electrodes in the LOC device enables the visualization of the entire cell monolayer. TEER was measured every day. Upon reaching the 6th day, a constant circulation of culture medium was introduced by a peristaltic pump (Masterflex, Cole-Parmer, USA) at 1 ml/min flow rate (0.4 dyne/cm^2) for 24 hours for the model in dynamic conditions. A higher, physiological shear stress (1.6 dyne/cm^2) was also tested in the model by the combination of increased medium viscosity (3.5% dextran) and an elevated, 2.5 ml/min flow rate. Under our experimental conditions the flow in the channel was laminar based on the Reynolds' number. Co-cultures in static conditions were kept as shown in Supplementary Figure S1. Right after this 24-hour static and dynamic condition we performed barrier integrity studies on the human BBB model, did RNA extraction of BLECs, stained for selected BBB proteins and glycocalyx related molecules and measured the surface charge of BLECs.

Barrier integrity measurement: transendothelial electrical resistance and permeability

Cells were kept in co-culture for 7 days and TEER values were recorded daily. The TEER was measured as described in our previous work[5]: the LOC electrodes were connected to the EVOM[2] voltohmmeter and the TEER values were registered (Figure 1(c)). To assess the barrier integrity small molecular weight marker Lucifer yellow (LY, MW: 457 Da)[18] and Evans blue dye bound to 1 % bovine serum albumin (EBA, MW: 67.5 kDa)[5] were used. Medium in the upper compartments of the LOC devices was replaced with 150 µl of Ringer-Hepes solution containing LY (5 µM) and EBA (165 µg/ml dye bound to 1 % albumin). In the bottom compartments 350 µl of Ringer-Hepes solution was added. LOCs were incubated for 20, 40 and 60 minutes in a CO_2 incubator at 37 °C on a horizontal shaker (150 rpm/min). Samples were collected from both compartments and fluorescent intensity measured by spectrofluorometer (Horiba Fluorolog 3, Japan). For details of the permeability assay and calculation of apparent permeability coefficients (P_{app}), see Supplementary Methods.

Immunohistochemistry

Cells were fixed with ice cold methanol and acetone solution (1:1) for 2 minutes, washed twice with phosphate buffered saline (PBS) containing 1% FBS and blocked with 3 % BSA in PBS for 1 hour. BLECs were incubated with primary antibodies for β-catenin, claudin-5, ZO-1, P-glycoprotein (PGP), glucose transporter-1 (GLUT-1), ICAM-1, VCAM-1 diluted in 3 % BSA-PBS blocking buffer and incubated overnight at 4 °C. Cells were washed in PBS and incubated with secondary antibody anti-rabbit IgG-CY3 or anti-mouse IgG Alexa-488 and H33342 dye for 1 hour. The same protocol was used to stain brain PCs for α-smooth muscle actin, NG2 and PDGFR-β. Alexa fluor 488 anti-mouse IgG, anti-rabbit IgG-CY3 were used as secondary antibodies. Samples were visualized by a Leica TCS SP5 confocal laser scanning microscope. For more details, see Supplementary Methods.

Massive analysis of cDNA ends library preparation and RNA sequencing

RNA isolation and RNA integrity analysis were performed as described in Supplementary Methods. Genome-wide gene expression profiling was performed using massive analysis of cDNA ends (MACE-seq) with RNA extracted from BLECs co-cultured with PCs in static and dynamic conditions (3 and 5 biological replicates, respectively). A total of 8 libraries were constructed using the Rapid MACE-Seq kit (GenXPro GmbH, Frankfurt, Germany), according to the manufacturer's protocol. MACE-seq performs gene

expression profiling by sequencing part of the 3' end of mRNA transcipts. While synthetizing one cDNA molecule from each mRNA transcript, MACE-seq can accurately quantify transcribed polyadenylated transcripts. For more details, see Supplementary Methods and Figure S2.

Bioinformatic analysis of MACE-seq data

Approximately 62 million MACE-seq reads were obtained across all 8 libraries, and subsequently processed and analyzed bioinformatically. PCR-duplicates were identified using the TrueQuant technology and subsequently removed from raw data. The remaining reads were further poly(A)-trimmed and low-quality reads were discarded. In the following step, the clean reads were aligned to the human reference genome (hg38, http://genome.ucsc.edu/cgi-bin/hgTables) using bowtie2 mapping tool resulting in a dataset of 28,834 different genes. The gene count data was normalized to account for differences in library size and RNA composition bias by calculating the median of gene expression ratios using DESeq2 R/Bioconductor package.[19] Testing for differential gene expression was also performed using the DESeq2 R/Bioconductor package. As a result, p-value and log2(fold change) (log2FC) were obtained for each gene in the dataset. False discovery rate (FDR) analysis was estimated to account for multiple testing. The gene expression level was calculated for each gene using the normalized value for the dynamic condition divided by the normalized value for the static condition multiplied by 100. Genes with a p-value < 0.05 and |log2FC| > 1 were considered to be differentially expressed. To perform functional profiling analysis g:Profiler was used to identify over-represented biochemical pathways from 3 databases (KEGG, Reactome and Gene Ontology) and to calculate the statistical significance of each pathway. GOplot was used to calculate the zscore from each over-represented pathway.[20] The transcriptomic datasets generated and analyzed in this study are available in the Gene Expression Omnibus (GEO) repository.[21] GEO accession number is GSE155671 and will also be available at the BBBHub (http://bbbhub.unibe.ch).

Zeta potential measurements

The zeta potential reflecting the surface charge of brain endothelial cells was measured by laser Doppler velocimetry using a Zetasizer Nano instrument (Malvern Instruments, UK) equipped with a He-Ne laser (λ=632.8 nm) as described previously.[16] For more details, see Supplementary Methods.

Staining of cell surface glycocalyx

After 24-hour dynamic and static condition BLECs in co-culture with PCs were washed with Ringer-Hepes buffer and fixed by 1 % paraformaldehyde in PBS for 15 min at room temperature. Following fixation cells were washed with PBS twice. BLECs were not permeabilized to ensure only surface labeling. Labeling of sialic acid and N-acetyl-D-glucosamine residues within the glycocalyx was done using wheat germ agglutinin lectin (WGA) conjugated with Alexa fluor 488 (W11261, Invitrogen) diluted at 5 µg/ml concentration in PBS and incubated for 10 min at room temperature.[22] Then non-specific binding sites on cells were blocked with 3% bovine serum albumin-PBS for 30 min at room temperature. Labeling for chondroitin sulfate was performed with an anti-chondroitin sulfate mouse monoclonal primary antibody (Merck, Germany; 1:100; AB_476879) overnight in 3% BSA-PBS buffer at 4 °C. The next day cells were washed in PBS and incubated with an anti-mouse-Alexa Fluor 488 secondary antibody (Life Technologies, USA, 1:400) for 1 h at room temperature. Pictures were taken with Leica TCS SP5 confocal laser scanning microscope at random positions, at least 14 images for each membrane. For each condition three independent experiments were performed. Fluorescent images were analyzed for staining intensity using the FIJI (ImageJ) software.

Statistics

Data are represented as means ± SD. To test the statistical significance between different groups, data were analyzed with unpaired t-test or one-way ANOVA followed by Bonferroni post-test using the GraphPad Prism 5.0 Software (GraphPad Software, USA). Results were considered statistically significant at p-values < 0.05. Experiments were repeated at least twice and a minimum number of 3 biological parallels were used.

Results

Human BBB model in the LOC device: effect of flow on barrier properties

The human BBB model has been characterized and comparisons of BLECs in monoculture vs. co-culture with brain pericytes were described in static culture conditions.[18,23] Our first goal was to optimize and characterize this human BBB model in the LOC device under flow. The LOC has two fluid compartments, similarly to culture inserts: a porous PET membrane separates the top and bottom channels (Figure 1(a) and 1(b)). One of the biggest advantages of the LOC compared to the cell culture insert setup

is the possibility of applying fluid flow to induce shear stress to mimic more physiological conditions for brain EC cultures.[5] As in the case of cell culture inserts,[18,23] BLECs were added to the top compartment, and brain PCs were seeded to the bottom compartment (Figure 1(b)). During the first 6 days feeding was applied every 8 hours (Supplementary Figure 1), followed by a 24-hour dynamic condition (flow rate: 1ml/min; 0.4 dyne/cm^2; Figure1(c)). For the static model 7 days of automatic feeding was used and no fluid flow was applied. The tightness of the barrier, which reflects the permissiveness of the monolayer for the passage of ions and molecules was characterized by measurement of TEER and permeability for LY and EBA.[5] As shown in Figure 1(e) 24-hour fluid flow elevated the TEER significantly by 18% (361.8 ± 166.3 $\Omega \times$cm^2 to 425.5 ± 188.8 $\Omega \times$cm^2). The paracellular permeability for LY was significantly decreased after fluid flow by 78% (16.3 ± 3.6 to 3.6 ± 1.4 × 10^{-6} cm/s) similarly to permeability for EBA, which was significantly decreased by 93% (1.77 ± 0.02 to 0.14 ± 0.01 × 10^{-6} cm/s) after dynamic condition (Figure 1(f). The morphology of BLECs also changed after dynamic as compared to static condition. After flow a more elongated cell shape was visible (Figure 1(d)) than in cells under static condition. When the barrier integrity of the BLEC/PC model was compared in the 0.4 *vs*. 1.6 dynes/cm^2 shear conditions, no difference was observed between the permeability or TEER values of the two groups in dynamic conditions (Figure S3 (b-c)).

Transcriptomic profile of the human BBB model: effect of flow on the global gene expression profile

To further characterize the effect of fluid flow on the human BBB co-culture model, we analyzed the transcriptomic gene expression profile of BLECs using the MACE-seq. Gene expression profiling analysis was able to detect expression from 28,807 different genes (Supplementary Figure S4(a)). A total of 396 genes had a p-value lower than 0.05 and an |log2FC| >1, which were considered differentially expressed (Figure 2(b)). From all the expressed genes, 174 (0.6%) and 222 (0.8%) were up and down regulated, respectively (Figure 2(a)). Using more stringent thresholds of |log2FC| >2 or <-2, 67 (0.2%) upregulated and 73 (0.3%) downregulated genes were identified, respectively. Hierarchical clustering and principal component analysis (PCA) were used to assess relatedness between samples (supplementary Figure 4(a) and (b)). PCA and clustering analysis grouped the expression profiles from dynamic and static condition in two separate clusters. Many of the top 50 differentially expressed, up- or downregulated genes

(Supplementary Table S1-S3) are related to cell adhesion, basal membrane composition, surface glycocalyx, enzymatic or transport processes at the BBB, which we discuss in the relevant sections below.

Transcriptomic gene expression profile of the human BBB model: effect of flow on endothelial cell markers

During the analysis of MACE data, we first wanted to verify the influence of fluid flow on the expression of general endothelial marker and other endothelial cell-related genes. Several basic endothelial marker genes were expressed in BLECs, including von Willebrand factor (VWF), vascular endothelial growth factor genes (VEGFA, B, C) and their receptors (VEGFR1-3), angiopoietins (ANGPT1, -2), endothelial cell specific molecule 1 (ESM1) and endothelial nitric oxide synthase (NOS3), as expected. However, many of these genes were not changed by flow (Figure 3(a)). Among the endothelial genes 24-hour flow significantly upregulated endothelin 1 (EDN1), nitric oxide synthase interacting protein (NOSIP) and vascular endothelial growth factor receptor 1 (VEGFR1) (Figure 3(a)) and significantly (13-fold) downregulated the lymphatic vessel endothelial marker gene LYVE1 to a very low expression level. In dynamic condition among the adhesion molecules (Figure 3(b)), the expression of intercellular adhesion molecule-1 gene (ICAM1) was significantly elevated. Other surface molecules were not changed by flow, such as adhesion regulating molecule-1 (ADRM1), activated leukocyte cell adhesion molecule (ALCAM), ICAM2, E- and P-selectins (SELE, -P) and vascular cell adhesion molecule-1 (VCAM1). Flow had no effect on endothelial cytoskeleton genes in the human BBB model, including actinins (ACTN), filamin (FLN), talin (TLN), tensin (TNS), vinculin (VCL) and vimentin (VIM), while significantly increased the expression of α-actinin-1 (ACTN1) and the actin cross-linker transgelin (TAGLN) genes. Importantly, genes for several members of the integrin family, especially α-subunits (ITGA5, -11, -E, -V) were overexpressed after flow (Figure 3(b)), along with a number of brain endothelial basal membrane genes like collagen type IV (COL4A1), as well as fibulin 5 (FBLN5), FNDC3B and members of the matrix metallopeptidase family (MMP1, -2, -10, -14) (Figure 3(c)). From the members of the ADAM (a disintegrin and metalloproteinase) family expressed in the human BBB model only one gene, ADAM-12 was upregulated by flow. Several basal membrane genes were unchanged by flow, including dystrophin (DMD), elastin (ELN), perlecan or basement membrane-specific heparan sulfate proteoglycan core protein (HSPG2), laminins (LAM) and vitronectin

(VTN). The significant upregulation of genes for cytoskeleton proteins, integrins and basal membrane molecules indicates pathways leading to better attachment of the cell layer at the abluminal side and demonstrates the importance of dynamic conditions for BBB models to better mimic physiological conditions *in vitro.*

Transcriptomic gene expression profile of the human BBB model: effect of flow on BBB-related genes

Three main junction groups participate in the formation of BBB: tight junctions (TJ), adherens junctions (AJ) and gap junctions (GJ).[25] These intercellular connections enable brain endothelial cells to form a dynamic interface between the blood and CNS.[6] Several TJ transmembrane or linker proteins were present at an unchanged level after the dynamic condition, including endothelial cell-selective adhesion molecule (ESAM), occludin (OCLN), claudin-12 (CLDN12), junctional adhesion molecule 3 (JAM3), MARVELD1 and -D2, zonula occludens protein-1 and -2 (TJP1 and TJP2) (Figure 4(a)). The gene expression level of JAM1, as well as that of CLDN1, -3, -5 and -7 were decreased after flow condition (Figure 4(a)). Among AJ proteins the gene expression level of vascular endothelial or VE-cadherin (CDH5), neuronal or N-cadherin (CDH2), nectin-2 and -3, α- and β-catenins (CTNNA1, -B1) remained unchanged, while the expression–levels of protocadherins-1 and -9 (PCDH1, -9) genes increased. Genes for gap junction proteins, known to be involved in intercellular communication and the regulation of TJs and AJs, connexin 43 (GJA1) and connexin 40 (GJA5) were significantly upregulated by dynamic condition (Figure 4(a)).

Active efflux pumps and drug metabolizing enzymes represent another line of defense at the level of BBB by providing protection against toxic chemical compounds. As shown in Figure 4(b) the gene expression level for many of the important ATP cassette binding (ABC) and other transporters participating in drug and metabolite efflux was unchanged after flow condition: ABCB1 (PGP), ABCG2 (breast cancer resistance protein, BCRP), members of the ABCC family (ABCC1-6 or MRP1-6) and the excitatory amino acid transporter-3 belonging to the solute carrier (SLC) family (SLC1A1/EAAT3). Other transporters, like the lipid transporters ABCA3 and ABCA8, expressed in both peripheral and brain tissues, were significantly downregulated after the dynamic condition along with the organic anion-transporting polypeptide 1 (SLCO4A1/OATP1) and the organic cation transporter-2 (SLC22A5/OCTN2). The only drug efflux transporter which gene was upregulated by flow was SLC22A5 (OCTN1). The

cytochrome (CYP) P450 enzymes, which participate in steroid and drug metabolism (so called drug metabolism phase I enzymes) and thus contribute to subsequent efflux of conjugated drugs at the level of BBB, are expressed in different barrier culture models.[26] Many members of the CYP family were expressed in the human BBB model and CYP1A1 and CYP1B1 genes were significantly overexpressed after flow (Figure 4(b)). Additionally, drug metabolism phase II enzymes of the BBB, epoxide hydrolase-1 (EPHX1) and glutathione S-transferase π (GSTP1) were also upregulated by flow (Figure 4(b)).

SLCs including glucose, monocarboxylate, amino acid and peptide transporters were expressed either with an unchanged level or were significantly overexpressed after flow in BLECs, except for SLC7A5/LAT1, which was downregulated (Supplementary Figure S5(a)). Among ion transporters and channels expressed at the BBB,[1] two ion transporter genes were upregulated, while potassium channel genes were downregulated by flow condition (Supplementary Figure S5(b)). The gene expression of many important BBB receptor genes was unchanged, except LRP3 and LRP5 which were increased and LDLRAD3, very low-density lipoprotein receptor (VLDLR) and caveolin-1 (CAV1) which were decreased (Supplementary Figure S5(b)).

We characterized the BLEC/PC model and verified the changes caused by flow for selected BBB proteins by immunostaining (Figure 5). Brain pericytes stained for α-smooth muscle actin and NG2 and showed a uniform morphology throughout all experiments (Figure 5(a)). In the MACE study we found lower expression levels for CLDN5 after fluid flow, while in the fluorescence intensity evaluation we observed a tendency of decrease for claudin-5 immunostaining, but no significant change (Figure 5(b)). Flow did not change the expression of β-catenin and ZO1 genes which was supported by the analysis of immunostaining for these junctional associated proteins (Figure 5(c-d)). Similar findings were observed for PGP and GLUT1 gene expression and immunostaining, where no change was seen (Figure 5(e-f)). The ICAM1 adhesion molecule gene expression was elevated after fluid flow, which was corroborated with the image analysis of the staining (Figure 5(g)). In the case of VCAM-1 flow did not alter its expression neither at gene nor at protein level (Figure 5(h)). The immunostaining for claudin-5 and β-catenin was also compared between the two dynamic conditions, and in the higher shear group a decreased fluorescent intensity was found for the immunostaining of both junctional proteins in comparison with the 0.4 dynes/cm^2 conditions (Figure S2 (d-f)).

Effect of flow on the human BBB model: endothelial surface charge and glycocalyx

The endothelial surface glycocalyx (ESG) plays an important role in the mechano-sensing and transduction functions of endothelial cells, which are essential to maintain vascular integrity and homeostasis.[10] ESG is a rich layer of carbohydrates connected through proteoglycans and glycoproteins to the surface of ECs (Figure 6(a) and (b)).[27] Most of the *in vitro* BBB models based on cell culture inserts lack fluid flow, therefore represent a static environment. While the importance of the ESG and extracellular matrix are in general acknowledged as elements of the defense system of the BBB, this is an under researched area. This is the reason why we aimed to investigate the transcriptomic gene expression changes of the surface glycocalyx and the extracellular matrix components after static and dynamic conditions of BLECs co-cultured with PCs in our LOC. As shown in Figure 6(c), glycocalyx core proteins, like decorin (DCN), glypican-1 (GPC1), syndecan-2 (SDC2) and versican (VCAN) genes were significantly upregulated in the dynamic condition. Other ESG core protein genes like biglycan (BGN), CD44, and other syndecans (SDC1, -3, -4) were also present, but their expression levels were not changed by flow. Four types of galectins that bind specifically to β-galactoside sugars within the glycocalyx were expressed in BLECs (GAL1, -3, -8, -9), of which the GAL3 gene was decreased by flow (Figure 6(c)). The human BBB model expressed a large number of enzymes which participate in the synthesis and remodeling of the ESG (Figure 6(c)). The genes of four enzymes, the carbohydrate sulfotransferase-1 (CHST1), heparanase (HPSE), hyaluronidase-2 (HYAL2) and the heparan sulfate 6-O-endosulfatase SULF2, which selectively removes 6-O-sulfate groups from heparan sulfate, were found to be upregulated by flow, while the expression of only one enzyme, β-1,4-galactosyltransferase-5 (B4GALT5) decreased. The expression changes in the ESG core proteins and galectins were caused by flow, since the effect of co-culture with PCs in static conditions did not induce such changes (Supplementary Figure S6(a)).

Brain EC glycocalyx is one of the thickest within the vasculature[12] and also cultured brain ECs have highly negative surface charge.[16] The main sources of this negative charge are the lipid head groups of the plasma membrane and the ESG, composed of highly negatively charged polysaccharide chains. Since ESG related genes were upregulated by flow, zeta potential measurement was performed to determine if the changes at gene expression influence the absolute value of the surface charge of BLECs. We measured a significant decrease in surface charge of BLECs (Figure 6(d)) in dynamic

condition (-12.4 ± 1.4 mV) compared to static condition (-11.0 ± 1.0 mV). We also compared the effect of co-culture with PCs in static conditions using cell culture inserts, and found that the negative surface charge of BLECs in the co-culture model decreased (-11.7 ± 1.2 mV) compared to the monoculture (-10.6 ± 1.4 mV) (Supplementary Figure 6(b)), indicating the importance of both flow and co-culture in the negative surface charge of brain ECs.

The more negative surface was related to a denser ESG as confirmed by the fluorescently labelled WGA lectin staining: a 50% increase in the fluorescence intensity was observed in the confocal images after 24-hour flow (Figure 6(e) and (g)). A 30% increase in WGA lectin staining was also observed in BLECs in co-culture with PCs as compared to monocultures in static conditions (Supplementary Figure S6(c) and (d)). The BLECs were immunolabeled for the surface glycosaminoglycan chondroitin sulfate (CS), but no change was found in the fluorescence intensity of the immunocytochemistry (Figure 6(h) and (f)). When we analyzed the staining for the sialic acid residues of the ESG by WGA lectin we saw no difference between the lower and the higher shear stress groups (Figure S2 (h and i)). Moreover, the zeta potential in the two dynamic groups was also not different from each other (Figure S2 (g)).

The effect of flow on the ESG was corroborated by the gene enrichment profiles (Figure 7). We found that the most significantly upregulated pathways after the introduction of flow conditions were the extracellular matrix and structure pathways and ESG related pathways.

Discussion

RNA sequencing analysis provided new data on mouse brain EC transcriptomics[7] and on zonation of ECs in mouse brain vasculature.[8] Culture models of the BBB in static condition have also been characterized at the transcriptomic level[26,28] including the BLEC model we use in the present study.[23] We found one study on the effect of fluid flow on the transcriptome of a human cell-based BBB model,[4] but no study analyzed transcriptomic changes of a human BBB model in an LOC-based system in dynamic condition yet.

The BBB is composed of brain ECs that have strong interaction with the neighboring astroglia endfeet and pericytes. Brain pericytes share a common basal membrane with the ECs and they have an important role in the development, maintenance, and regulation of BBB functions.[1,29] Co-culture of brain ECs with PCs is

known to elevate the tightness of the paracellular barrier and increase the BBB properties.[18,30,31] The human BBB model used in our study, in which hECs are derived from hematopoietic stem cells and co-cultured with bovine brain PCs, is a well characterized *in vitro* model.[18,23,32] There is only one recent study which describes the adaptation of this BBB model to the use of short-term (4 and 30 minutes) fluid flow with the goal to study immune cell transmigration.[32] However, no longer term (24-hour) fluid flow and its effects on this BBB model have been investigated until now.

We evaluated the effects of two dynamic conditions on the BBB model in the LOC device, a 0.4 dynes/cm^2 shear stress and a four-times higher, 1.6 dynes/cm^2 condition, that can be considered as physiological, typical for postcapillary venules in the brain. To sum up our observations, we can conclude that the higher shear condition was well-tolerated by the BLECs, and it was similarly beneficial to the barrier integrity elevation and glycocalyx expression as the lower shear condition. We acknowledge that the 0.4 dynes/cm^2 shear is lower than that in brain microvessels *in vivo*, which is a limitation of the study. However, based on our data, this lower shear stress provided sufficient dynamic condition for the BLEC model to observe improved barrier integrity and the expression of important BBB genes and characteristics. The characterization of a human co-culture BBB model under static and dynamic conditions in an LOC device and the global transcriptomic gene expression analysis may provide valuable data to further improve BBB LOC models.

First, we measured the barrier properties of the BLEC and bovine PC co-culture model in the LOC device. In static conditions in the device similar TEER values were obtained for this human BBB model as for several types of *in vitro* co-culture models, including primary cell based ones.[26] After introducing fluid flow, TEER values significantly increased and permeability of the BLEC monolayers significantly decreased for both LY and EBA markers. Similar changes were found by previous studies using human BBB culture models in LOC devices.[4,5] The permeability values obtained for the marker molecule LY in dynamic conditions in the LOC device was lower than those in previous studies using culture inserts representing static conditions.[18,32] In contrast to the dynamic *in vitro* system using hollow fiber cartridges[4] our LOC device[5] allowed the morphological observation of BLECs, which showed similar immunostaining of junctional proteins as in the culture insert models.[18,32] Fluid flow changed cell shape to be more elongated and also realigned the cells in the direction of flow, in accordance with a previous study on bovine brain endothelial cells.[33] These observations prove, that the

LOC device is functional and show the importance of fluid flow in barrier integrity regulation of *in vitro* human BBB models.[4,5]

Blood flow in capillaries and the resulting shear force are important physiological regulators of EC functions in the periphery[10] and in the brain.[1] Many *in vitro* BBB models are based on culture inserts, therefore lack fluid flow.[26] Hollow fiber cartridges[4], microfluidic LOC devices[3,34] as well as bioengineered cerebral vessels[35] allow the study of fluid flow on BBB models. Different flow models are used for different studies. A linked organ-on-chip model of the human neurovascular unit revealed the metabolic coupling of endothelial and neuronal cells,[34] while a bioengineered model of human cerebral arteries was used to study the molecular mechanism of cerebrovascular amyloid angiopathy.[35] Flow-mediated regulation of endothelial genes has been studied on vascular ECs for a long time. Upregulation of genes TGF-β, EDN1/ET-1, CCL2/MCP-1 and ICAM-1 has been described previously[36] and we confirmed these data in the present study. The observed changes in our BBB model are complex: while expression level of the vasoconstrictor EDN-1 gene was increased, the level of one of its receptor gene, EDNRB, was decreased, and the vasodilating factor NOSIP, which interacts with NOS3, was found to be significantly upregulated. VEGFR1, upregulated by flow in our model, mediates endothelial cytoprotection via serine/threonine-specific protein kinase AKT/protein kinase B.[37] LYVE-1 expression is extremely low or null in mouse brain capillary derived ECs.[8] The hematopoietic stem cell-derived hECs in monoculture show general endothelial cell properties, then they are differentiated into BLECs by the co-culture with brain PCs. We found that BLECs in static conditions expressed LYVE1 gene at low level, which was reduced by 13-fold to a very low expression level in dynamic conditions indicating that more BBB-like properties were induced in the LOC device.

Among EC surface adhesion molecules flow elevated the expression of ICAM1 gene, as described in the case of vascular ECs[36] and a human BBB model[4] which can be important for immune cell transmigration studies.[32] We should note that the gene expression level of ICAM1 after upregulation in the dynamic setup was still low and at a similar level observed in mouse brain capillary derived ECs,[8] indicating there was no inflammatory stimulus. We found no change in the gene expression for several cell surface molecules including ICAM2, E and P-selectins. Our findings are in accordance with previous data on the BLEC model in static conditions.[23]

Endothelial cells respond to fluid flow by changing their morphology to a more elongated shape and align with the flow direction.[11] Our morphological findings on the

human BBB model in the LOC device are in accordance with these observations, and further supported by the upregulation of cytoskeletal genes ACTN1, known to interact with NOS3, and TAGLN, crosslinking actin filaments and participating in cytoskeletal reorganization. Flow is also known to increase the adhesion of ECs to the basal membrane via integrins, which interact with collagen, laminin, and fibronectin.[27] We found that several integrin-α subunit genes were significantly increased in dynamic conditions, while integrin-β subunits were unchanged or downregulated. In a human EC and astrocyte co-culture model an increase in the gene expression for both α and β integrin subunits was observed after flow,[4] which may indicate a special role for astrocytes in the induction of these genes. In our study the differentially expressed basal membrane genes COL4A1, FBLN5 and the fibronectin related FNDC3B together with integrins may indicate a stronger attachment of the cells in dynamic condition. MMPs are important in different physiological and pathological processes at the BBB. In cerebral ischemia MMPs participate in both the vascular injury and the repair phase during angiogenesis and reestablishment of blood flow.[38] In our study several MMPs were differentially expressed, and this upregulation may be related with basal membrane remodeling induced by flow.

The paracellular tightness of the BBB is controlled by transmembrane TJ proteins. We found the downregulation of epithelial claudins CLDN1, -3, -7 by flow. These claudins were also expressed at a low level in BBB culture models[26] and in isolated brain ECs.[7,8] Flow did not change the expression level of important TJ genes ESAM, OCLDN, JAMs, MARVELDs and linkers TJPs. The expression level of claudin-5 gene, considered as the most important claudin in brain ECs was decreased by flow in our co-culture model with PCs, which was not observed in the astrocyte co-culture model.[4] In contrast, the genes of adherens junction proteins were either unchanged or upregulated together with gap junction genes. These, together with the unchanged level of several TJ genes and increased level of basal membrane protein and integrin gene expression might explain that we observed an increased barrier integrity of the BBB model by functional measurements, namely TEER and permeability for marker molecules.

The chemical protection of the CNS is maintained by active efflux pumps, mainly ABC transporters, the gene expression level of which was mostly unchanged in dynamic condition. Enzymes participating in drug metabolism were more sensitive to the effect of flow, and their level was unchanged or upregulated like in the case of phase I enzymes CYP1A1 and CYP1B1, and phase II enzymes EPHX1 and GSTP1. The upregulation of

17

P450 enzymes in a human BBB model by fluid flow was also described.[4] The increased gene expression level of phase II enzymes EPHX1 and GSTP1 in brain ECs was also observed by co-culture with PCs.[23]

SLC transporters are key for the proper transport of nutrients to the CNS.[9] The expression level of SLC transporters was either unchanged or in many cases increased in dynamic conditions. In addition to nutrients, the BBB regulates the transport of ions by SLCs. On the human BBB model flow increased the gene expression of anion exchanger AE2 and the K^+- Cl^- cotransporter (KCC1). While the level of voltage dependent Ca^{2+} (CACN family) and anion (VDAC) channels was unchanged by flow, several K^+ channels were found downregulated, which were also expressed at a very low level in isolated brain capillary ECs.[8] In the human BBB co-culture model with astrocytes an upregulation of Ca^{2+} and K^+ channels was observed in dynamic conditions[4] indicating an important role for the co-culture conditions.

Many important proteins and peptides, like insulin and holotransferrin, cross the BBB by receptor-mediated pathway.[1] Flow did not change the expression level of many of these receptors. One of the exception is the gene of LRP5, a canonical WNT pathway signaling co-receptor, which was increased. Importantly, LRP5 participates in barrier genesis and BBB maturation.[1] Flow also downregulated in the human BBB model the expression level of caveolin-1 gene. Since isolated brain ECs express much less CAV1 than peripheral (lung) ECs,[8] these changes may point to barrier maturation in the present model. We confirmed the presence of several BBB related proteins in the BLEC model by immunostaining. In concordance with the gene expression data, no changes were found between the static and dynamic conditions for junctional associated molecules β-catenin and ZO-1, the efflux pump PGP, the glucose transporter GLUT1, and the adhesion molecule VCAM-1. We found lower gene expression levels for claudin-5 after fluid flow, while in the fluorescence intensity evaluation a tendency of decrease but no significant change was observed. Fluid flow elevated the gene expression of ICAM-1 adhesion molecule, which was corroborated with immunocytochemistry data.

The study of Cucullo et al. described transcriptomic changes in BBB-related genes induced by flow on a human BBB model,[4] but no data are available on the gene expression of mechano-sensing and luminal glycocalyx components. Continuous blood flow regulates the composition of ESG, the dynamic equilibrium of glycoproteins, proteoglycans, glycosaminoglycans and the associated plasma proteins.[27] ESG is not only important as an element of the physical barrier[15] with its highly negative charge but also

control the stability of endothelial cells. We observed the differential upregulation of major glycocalyx core protein genes DCN, SDC2 and VCAN, as well as an increase in GPC1 expression, which act as mechano-sensors and also link the ESG to the cytoskeleton, therefore actively participate in flow induced morphological changes in ECs.[10] The increased gene expression level of glycocalyx-related enzymes heparanase and hyaluronidase-2, as well as carbohydrate sulfotransferase-1 and the heparan sulfate 6-O-endosulfatase SULF2 adding and removing sulfate groups, which are important for the overall negative charge of the glycocalyx, may indicate active remodeling of the ESG in dynamic condition. Direct measurement of the surface charge of the ECs by a laser Doppler velocimetry confirmed that cells became more negatively charged. These data together with increased WGA lectin staining support that the ESG of the human BBB model became more robust. These observations are further corroborated that the three most enriched pathways in the human BBB model after flow were related to extracellular matrix organization, extracellular matrix structure organization and collagen-containing extracellular matrix. In addition, several other pathways related to cell surface, extracellular matrix proteoglycan and dermatan sulfate biosynthesis and metabolism were also increased.

In conclusion, flow increased barrier properties, induced several key general endothelial and BBB-related genes on BLECs in the LOC device. In addition, flow not only upregulated extracellular matrix and glycocalyx-related genes and pathways, but made the brain endothelial cell surface more negatively charged and more rich in lectin binding sites. These results strongly argue for the inclusion of flow in BBB models and draw the attention to the importance of the endothelial surface glycocalyx as an element of the BBB. This human model can be used as a tool to study the role of cell surface glycocalyx in BBB physiology and pathology.

Author contribution statement

Conceptualization, ARSM, FRW, MD; Methodology, ARSM, FRW, RF, AK; Formal analysis, ARSM, RF; Investigation, ARSM, FRW, RF, MH, AK; JV; Data curation, ARSM, FRW, RF; Writing - original draft preparation, ARSM, FRW, MD; Writing review and editing, ARSM, FRW, RF, AK, JV, MH, MC, PW, FG, AD, MD; Supervision, FRW, AD, PW, MC and MD; Funding acquisition, AD and MD.

Disclosure/conflict of interest

The authors declare that they have no conflicts of interest with the contents of this article.

Supplementary material for this paper can be found at http://jcbfm.sagepub.com/content/by/supplemental-data

References

1. Sweeney MD, Zhao Z, Montagne A, et al. Blood-Brain Barrier: From Physiology to Disease and Back. *Physiol Rev* 2019;99(1):21-78.

2. Helms HC, Abbott NJ, Burek M, et al. In vitro models of the blood-brain barrier: An overview of commonly used brain endothelial cell culture models and guidelines for their use. *J Cereb Blood Flow Metab* 2016; 36(5):862-890.

3. Raimondi I, Izzo L, Tunesi M, et al. Organ-On-A-Chip in vitro Models of the Brain and the Blood-Brain Barrier and Their Value to Study the Microbiota-Gut-Brain Axis in Neurodegeneration. *Front Bioeng Biotechnol* 2020; 7:435.

4. Cucullo L, Hossain M, Puvenna V, et al. The role of shear stress in Blood-Brain Barrier endothelial physiology. *BMC Neurosci* 2011; 12:40.

5. Walter FR, Valkai S, Kincses A, et al. A versatile lab-on-a-chip tool for modeling biological barriers. *Sensors and Actuators B: Chemical* 2016, 222: 1209-1219.

6. Abbott NJ, Patabendige AA, Dolman DE, et al. Structure and function of the blood-brain barrier. *Neurobiol Dis* 2010;37(1):13-25.

7. Daneman R, Zhou L, Agalliu D, et al. The mouse blood-brain barrier transcriptome: a new resource for understanding the development and function of brain endothelial cells. *PLoS One* 2010; 5(10):e13741.

8. Vanlandewijck M, He L, Mäe MA, et al. A molecular atlas of cell types and zonation in the brain vasculature. *Nature* 2018;554(7693):475-480.

9. Campos-Bedolla P, Walter FR, Veszelka S, et al. Role of the blood-brain barrier in the nutrition of the central nervous system. *Arch Med Res* 2014;45(8):610-638.

10. Fu BM and Tarbell JM. Mechano-sensing and transduction by endothelial surface glycocalyx: composition, structure, and function. *Wiley Interdiscip Rev Syst Biol Med* 2013;5(3):381-390.

11. Zeng Y, Zhang XF, Fu BM, et al. The Role of Endothelial Surface Glycocalyx in Mechanosensing and Transduction. *Adv Exp Med Biol* 2018; 1097:1-27.

12. Ando Y, Okada H, Takemura G, et al. Brain-Specific Ultrastructure of Capillary Endothelial Glycocalyx and Its Possible Contribution for Blood Brain Barrier. *Sci Rep* 2018; 8(1):17523.

13. Ribeiro MM, Domingues MM, Freire JM, et al. Translocating the blood-brain barrier using electrostatics. *Front Cell Neurosci* 2012; 6:44.

14. Hervé F, Ghinea N and Scherrmann JM. CNS delivery via adsorptive transcytosis. *AAPS J* 2008; 10(3):455-472.

15. Kutuzov N, Flyvbjerg H and Lauritzen M. Contributions of the glycocalyx, endothelium, and extravascular compartment to the blood-brain barrier. *Proc Natl Acad Sci USA* 2018;115(40):E9429-E9438.

16. Santa-Maria AR, Walter FR, Valkai S, et al. Lidocaine turns the surface charge of biological membranes more positive and changes the permeability of blood-brain barrier culture models. *Biochim Biophys Acta Biomembr* 2019;1861(9):1579-1591.

17. van den Berg BM, Nieuwdorp M, Stroes ES, et al. Glycocalyx and endothelial (dys) function: from mice to men. *Pharmacol Rep* 2006; 58 Suppl:75-80.

18. Cecchelli R, Aday S, Sevin E, et al. A stable and reproducible human blood-brain barrier model derived from hematopoietic stem cells. *PLoS One* 2014;9(6):e99733.

19. Love MI, Huber W and Anders S. Moderated estimation of fold change and dispersion for RNA-seq data with DESeq2. *Genome Biol* 2014;15(12):550.

20. Walter W, Sánchez-Cabo F and Ricote M. GOplot: an R package for visually combining expression data with functional analysis. *Bioinformatics* 2015;31(17):2912-2914.

21. Edgar R, Domrachev M and Lash AE. Gene Expression Omnibus: NCBI gene expression and hybridization array data repository. *Nucleic Acids Res* 2002; 30(1):207-210.

22. Betteridge KB, Arkill KP, Neal CR, et al. Sialic acids regulate microvessel permeability, revealed by novel in vivo studies of endothelial glycocalyx structure and function. *J Physiol* 2017;595(15):5015-5035.

23. Heymans M, Figueiredo R, Dehouck L, et al. Contribution of brain pericytes in blood-brain barrier formation and maintenance: a transcriptomic study of cocultured human endothelial cells derived from hematopoietic stem cells. *Fluids Barriers CNS* 2020;17(1):48.

24. Luu VZ, Chowdhury B, Al-Omran M, et al. Role of endothelial primary cilia as fluid mechanosensors on vascular health. *Atherosclerosis* 2018; 275:196-204.

25. De Bock M, Vandenbroucke RE, Decrock E, et al. A new angle on blood-CNS interfaces: a role for connexins? *FEBS Lett 2014*; 588(8):1259-1270.

26. Veszelka S, Tóth A, Walter FR, et al. Comparison of a Rat Primary Cell-Based Blood-Brain Barrier Model with Epithelial and Brain Endothelial Cell Lines: Gene Expression and Drug Transport. *Front Mol Neurosci* 2018;11:166.

27. Reitsma S, Slaaf DW, Vink H, et al. The endothelial glycocalyx: composition, functions, and visualization. *Pflugers Arch* 2007; 454(3):345-359.

28. Urich E, Lazic SE, Molnos J, et al. Transcriptional profiling of human brain endothelial cells reveals key properties crucial for predictive in vitro blood-brain barrier models. *PLoS One* 2012; 7(5):e38149.

29. Villaseñor R, Kuennecke B, Ozmen L, et al. Region-specific permeability of the blood-brain barrier upon pericyte loss. *J Cereb Blood Flow Metab* 2017; 37(12):3683-3694

30. Nakagawa S, Deli MA, Kawaguchi H, et al. A new blood-brain barrier model using primary rat brain endothelial cells, pericytes and astrocytes. *Neurochem Int* 2009; 54(3-4):253-263.

31. Thomsen LB, Burkhart A and Moos T. A Triple Culture Model of the Blood-Brain Barrier Using Porcine Brain Endothelial cells, Astrocytes and Pericytes. *PLoS One* 2015;10(8):e0134765.

32. Mossu A, Rosito M, Khire T, et al. A silicon nanomembrane platform for the visualization of immune cell trafficking across the human blood-brain barrier under flow. *J Cereb Blood Flow Metab* 2019;39(3):395-410.

33. Colgan OC, Ferguson G, Collins NT, et al. Regulation of bovine brain microvascular endothelial tight junction assembly and barrier function by laminar shear stress. *Am J Physiol Heart Circ Physiol* 2007; 292(6):H3190-H3197.

34. Maoz BM, Herland A, FitzGerald EA, et al. A linked organ-on-chip model of the human neurovascular unit reveals the metabolic coupling of endothelial and neuronal cells. *Nat Biotechnol*. 2018;36(9):865-874.

35. Robert J, Button EB, Martin EM, et al. Cerebrovascular amyloid Angiopathy in bioengineered vessels is reduced by high-density lipoprotein particles enriched in Apolipoprotein E. *Mol Neurodegen*. 2020;15(1):23.

36. Ando J and Kamiya A. Flow-dependent regulation of gene expression in vascular endothelial cells. *Jpn Heart J* 1996; 37(1):19-32.

37. Dragoni S and Turowski P. Polarised VEGFA Signalling at Vascular Blood–Neural Barriers. *Int J Mol Sci* 2018;19(5):1378.

38. Rempe RG, Hartz AMS and Bauer B. Matrix metalloproteinases in the brain and blood-brain barrier: Versatile breakers and makers. *J Cereb Blood Flow Metab* 2016; 36(9):1481-1507.
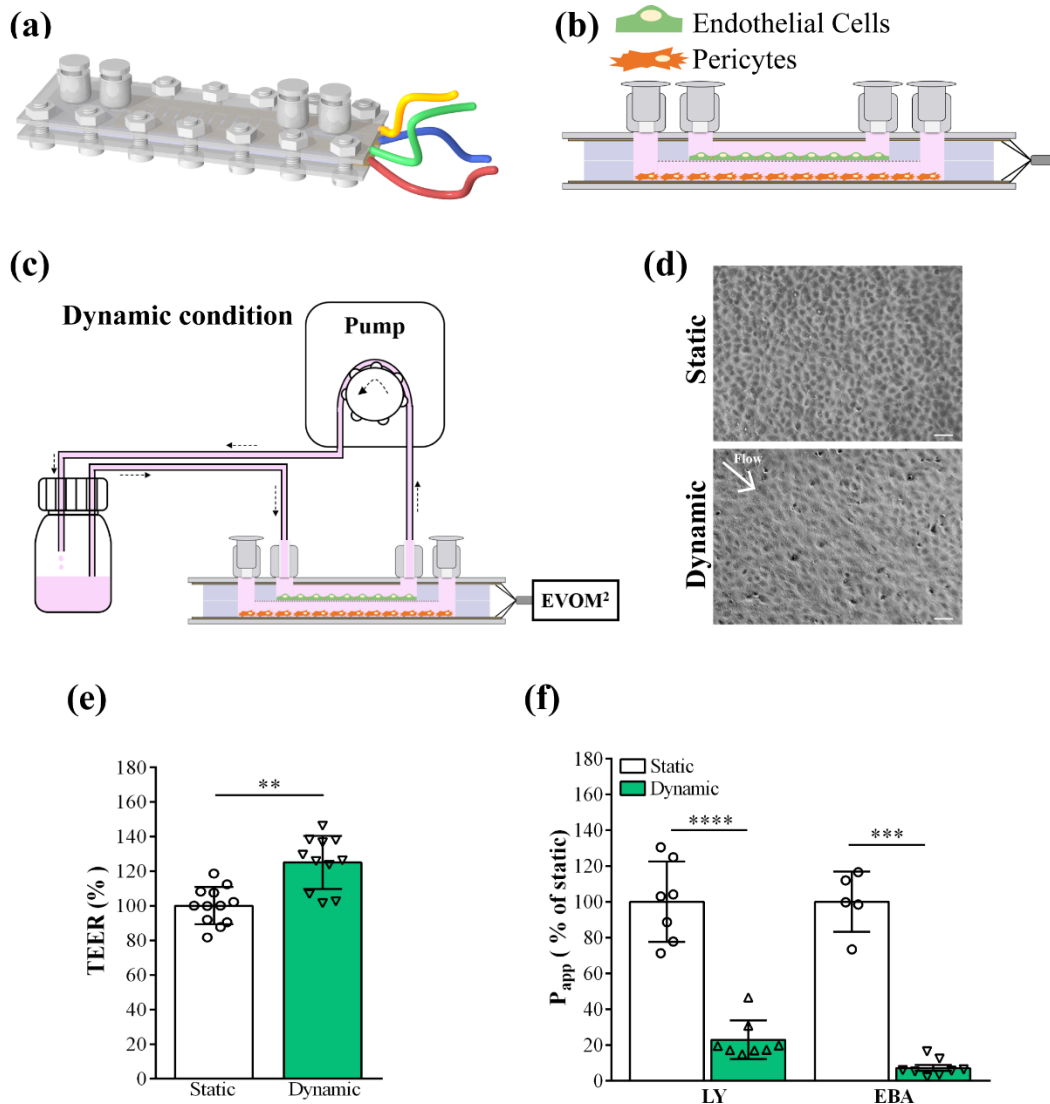
Figure legends

Figure 1. Characterization of the human BBB model cultured in the lab-on-a-chip (LOC). (a) Representative illustration of the device. The plastic slides carrying the gold electrodes to measure transendothelial electric resistance (TEER) are positioned at the top and bottom of the device, followed by the top and bottom channels made by PDMS and the cell culture membrane in the middle. The layers of the LOC were joined with screws. The female luer inlets were located on the top and provided easy access for both top and bottom channels. (b) Diagonal view of the LOC. Human brain endothelial cells were added to the top compartment, brain pericytes to the bottom. (c) Dynamic condition: the device was connected to a peristaltic pump and a reservoir containing cell culture medium. Fluid flow was applied at a speed of 1 ml/min for 24 hours. (d) Phase contrast images of brain endothelial cells under static and dynamic conditions. Scale bar: 20 μm. (e) TEER results were normalized to the values of the static condition which did not receive any fluid flow, values are presented as means ± SD, unpaired t-test, **p<0.01, n=12. (f) Apparent permeability coefficient (Papp) of the human BBB model under static and dynamic conditions, for Lucifer yellow (LY) and Evans blue labelled albumin (EBA) marker molecules. Data is shown as the % of the static condition and presented as means ± SD (unpaired t-test, *p<0.05, **p<0.01, n=5-8).
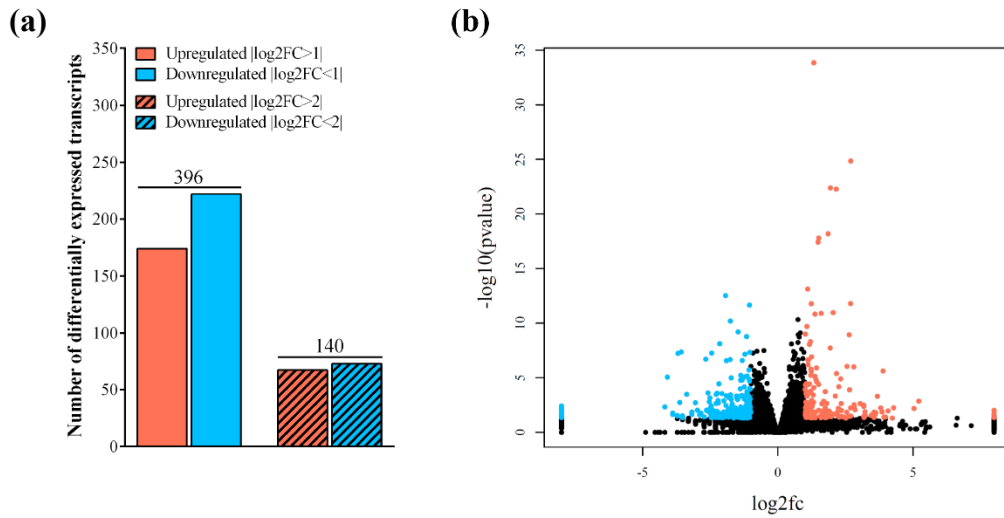
Figure 2. (a) Number of differentially expressed transcripts of human endothelial cells co-cultured with brain pericytes under dynamic and static conditions. The total number of differentially expressed transcripts are shown on top of the bars. Testing for differential gene expression was performed using the DESeq2 R/Bioconductor package.[19] (b) The volcano plot identifies the total changes in the data set. Black: no change, Blue: downregulated genes, Red: upregulated genes.
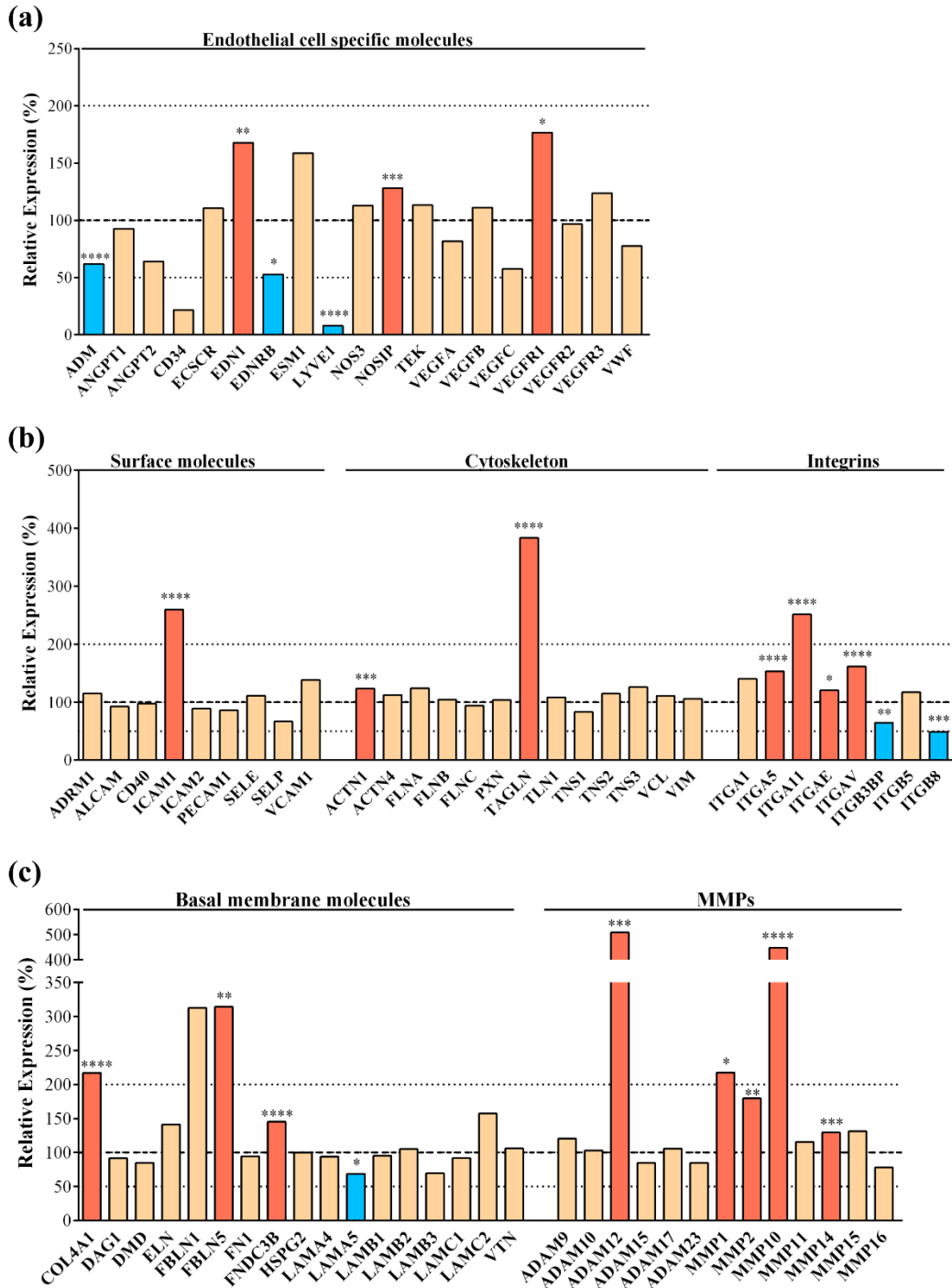
Figure 3. Transcriptomic gene expression profile of (a) Endothelial cell specific genes. (b) Endothelial cell surface molecules, cytoskeleton molecule and integrin genes; (c) Basal membrane molecule and matrix metalloproteinase (MMP) genes. Expression is shown as the relative expression (%) of the genes present in human endothelial cells co-cultured with brain pericytes in dynamic condition as compared to static condition. Testing for differential gene expression was performed using the DESeq2 R/Bioconductor package.[19] Genes with a p-value <0.05 and less than 50% or more than 200% gene expression levels were considered to be differentially expressed. Red color labels upregulation and statistically significant expression changes, blue color shows downregulation and statistically significant expression change, cream color indicates no change in the gene expression (*p<0.05, **p<0.01, ***p<0.001, ****p<0.0001).
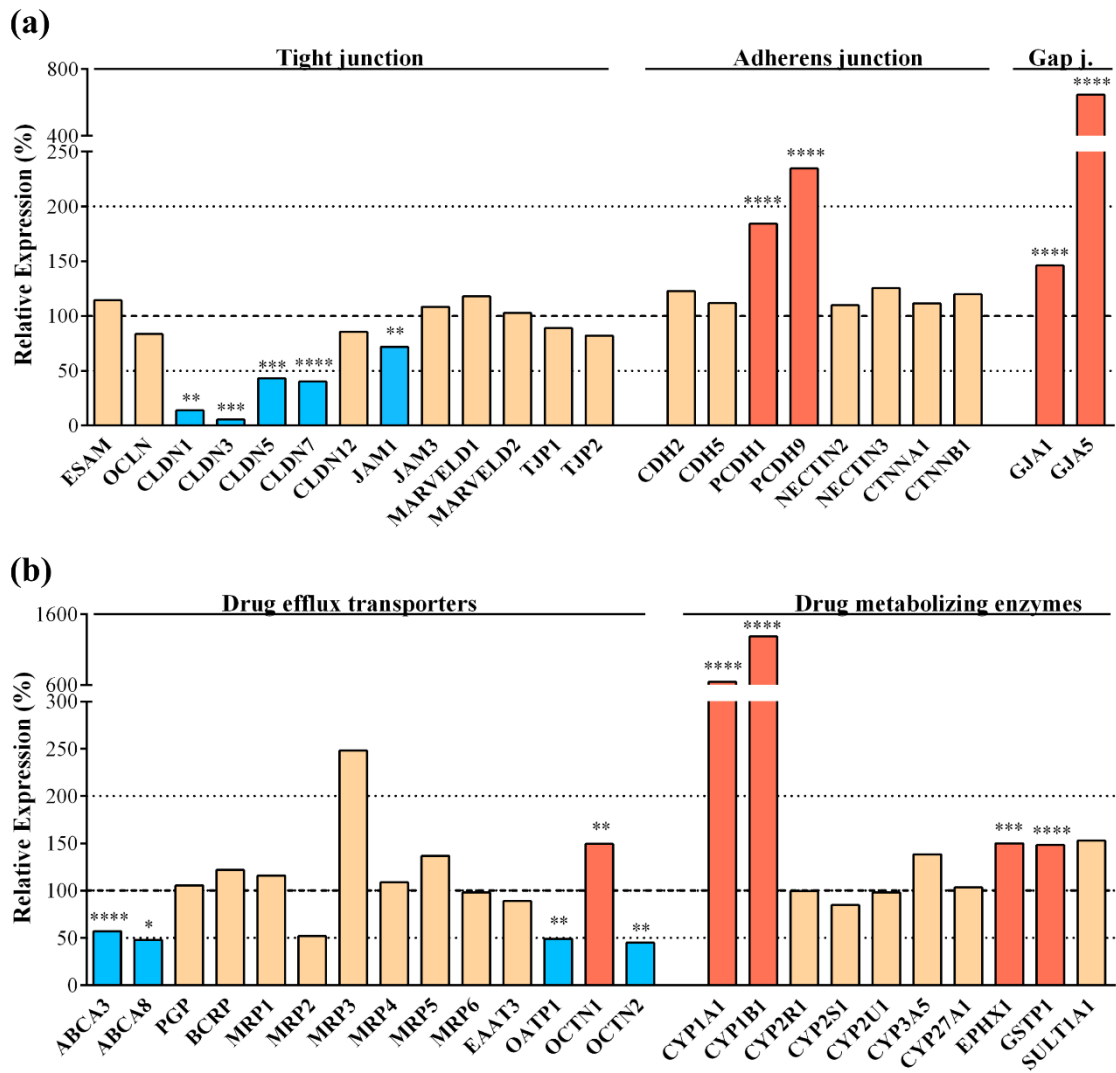
Figure 4. Transcriptomic gene expression profile of (a) tight, adherens and gap junction protein genes. (b) drug efflux transporter and drug metabolizing enzyme genes. Expression is shown as the relative expression (%) of the genes present in human endothelial cells co-cultured with brain pericytes in dynamic condition as compared to static condition. Testing for differential gene expression was performed using the DESeq2 R/Bioconductor package.[19] Genes with a p-value < 0.05 and less than 50% or more than 200% gene expression levels were considered to be differentially expressed. Red color labels upregulation and statistically significant expression changes, blue color shows downregulation and statistically significant expression change, cream color indicates no change in the gene expression (*p<0.05, **p<0.01, ***p<0.001, ****p<0.0001).
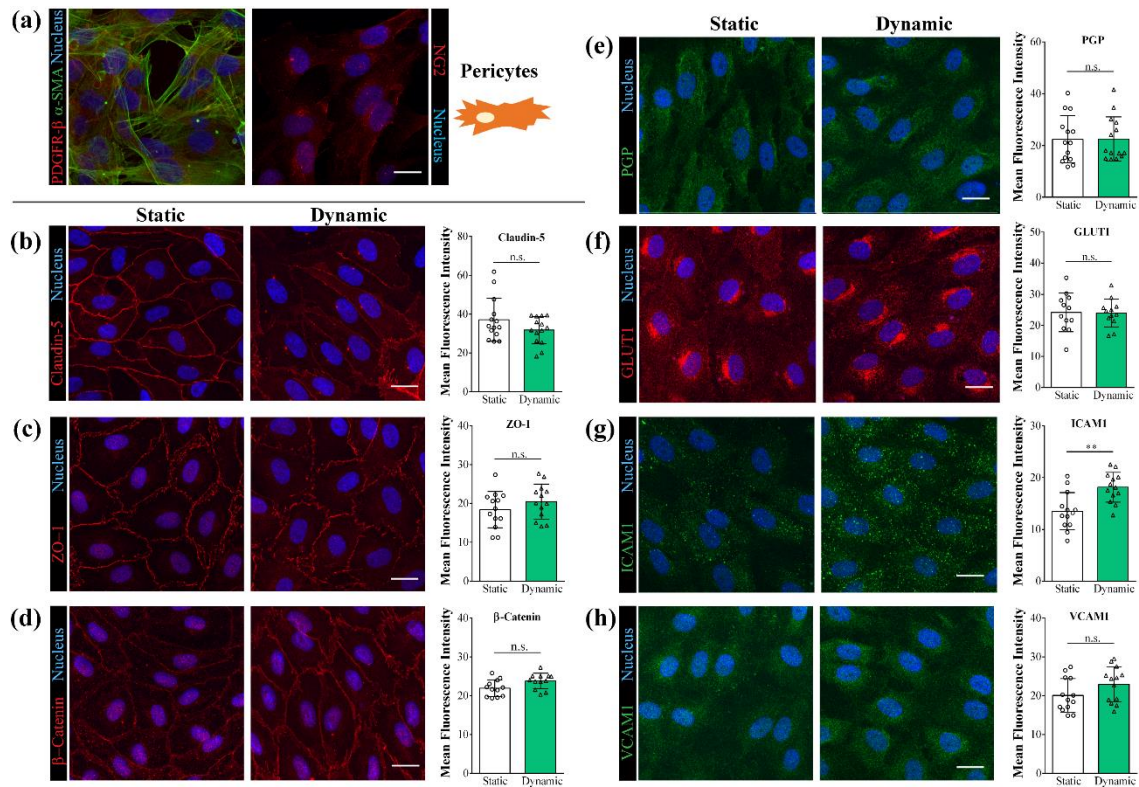
Figure 5. Immunocytochemistry of brain pericytes and human brain-like endothelial cells. (a) Brain pericytes were characterized by immunostaining for platelet-derived growth factor (PDGF)-β receptor, α-smooth muscle actin (α-SMA) and neuron-glial antigen 2 (NG2). Brain-like endothelial cells in static and dynamic conditions were characterized by immunostaining followed by fluorescence intensity evaluation (n=12-14) for: (a-c) junctional proteins claudin-5, zonula occludens – 1 and β-catenin; (e-f) efflux pump P-glycoprotein (PGP) and solute carrier glucose transporter-1 (GLUT1); (g-h) cell adhesion molecules intercellular adhesion molecule-1 (ICAM-1) and vascular cell adhesion molecule-1 (VCAM-1). Scale bar: 20 μm.
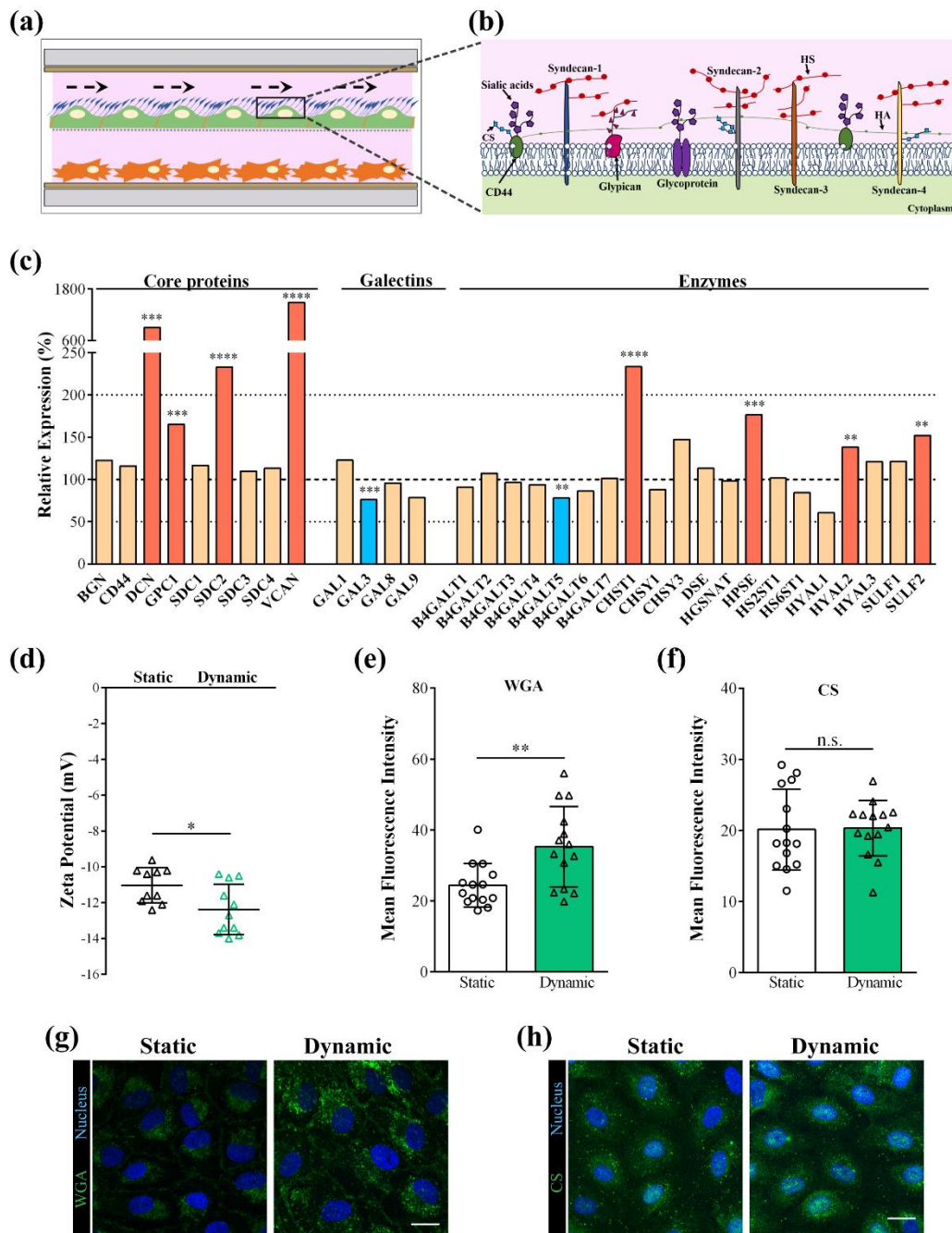
Figure 6. (a) Illustration showing the effect of fluid flow on the endothelial surface glycocalyx (ESG). (b) Drawing representing ESG core proteins, glycoproteins and glucosaminoglycans. HA: hyaluronic acid, HS: heparan sulfate, CS: chondroitin sulfate. (c) Transcriptomic gene expression profile of ESG-related genes. Expression is shown as the relative expression (%) of the genes present in human endothelial cells co-cultured with brain pericytes in dynamic condition as compared to static condition. Testing for differential gene expression was performed using the DESeq2 R/Bioconductor package.[19] Genes with a p-value < 0.05 and less than 50% or more than 200% gene expression levels were considered to be differentially expressed. Red color labels upregulation and statistically significant expression changes, blue color shows downregulation and statistically significant expression change, cream color indicates no change in the gene expression (*p<0.05, **p<0.01, ***p<0.001, ****p<0.0001). (d) Zeta potential measured by laser Doppler velocimetry (means ± SD, n=10; unpaired t-test, * p<0.05 compared to static condition). (e) and (f) Fluorescent intensity analysis of the images

showing wheat germ agglutinin (WGA) lectin staining and chondroitin sulfate immunocytochemistry. Image analysis values are presented as means ± SD, n=14 images/groups; unpaired t-test, **p<0.01 compared to static condition. (g) and (h) Staining of ESG on brain endothelial cells with fluorescently labeled WGA lectin that binds to the sialic acid residues and with chondroitin sulfate immunocytochemistry. Scale bar: 20 µm.
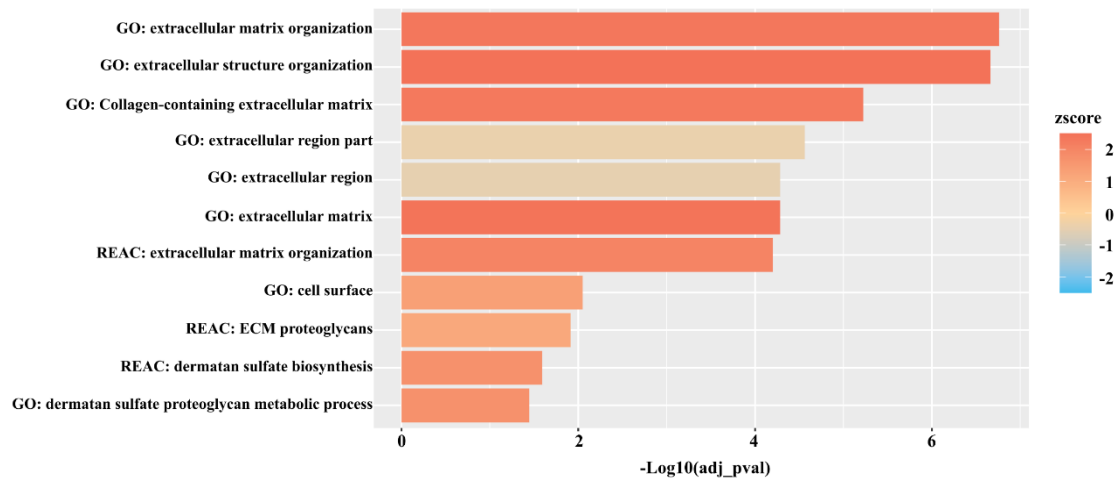

Figure 7. Functional profiling analysis of extracellular matrix-related pathways in static versus dynamic condition. The x-axis represents the statistical significance calculated using g:Profiler while the zscore represents the tendency of the regulation of these pathways calculated using GOplot.